Chemical Engineering Journal 155 (2009) 580–585

Contents lists available at ScienceDirect

Chemical Engineering Journal

journal homepage: www.elsevier.com/locate/cej

Sorption studies of ^{134}Cs, ^{60}Co and $^{152+154}Eu$ on phosphoric acid activated silico-antimonate crystals in high acidic media

Ismail M. Ali*

Nuclear Fuel Technology Department, Hot Labs. Centre, Atomic Energy Authority, P.C. 13759, Cairo, Egypt

ARTICLE INFO

Article history:
Received 9 April 2009
Received in revised form 24 July 2009
Accepted 28 July 2009

Keywords:
Silico-antimonate
Phosphoric acid activation
Sorption kinetics

ABSTRACT

This work describes the sorption of ^{134}Cs, ^{60}Co and $^{152+154}Eu$ by crystals of unmodified and phosphoric acid modified silico-antimonates (SiSb). Equilibrium and selectivity sequence for co-exiting metal ions under strongly acidic conditions of $HClO_4$, H_2SO_4, HNO_3 and HCl were investigated. The results showed that the silico-antimonate either in the high Sb^{5+} content or in the phosphated form possesses acidic characters and shows cation-exchange properties more efficient in acidic media. Kinetic studies indicated that pseudo-second-order model gave better fitting parameters comparing to that of pseudo-first-order one. The thermodynamic parameters of the sorption processes revealed spontaneous and endothermic nature. High negativity of ΔG° values for the modified SiSb confirms the positive role of phosphoric acid impregnation in the sorption process. The break-through capacities of the studied ions were further calculated from a column investigation.

1. Introduction

During the last few years, a wide application of inorganic ion exchangers in nuclear waste treatment has been investigated for fission and activation products elimination [1]. Most of the inorganic ion exchangers [2–4] such as lithium titanate, tin silicate, tin- and titanium-ferrocyanides, etc., exhibit very low ion exchange efficiency in the high acidic media. Considerable research has been carried out to study and develop acidic inorganic ion exchangers such as metal antimonates $M_xSb_yO_z{\cdot}wH_2O$ (M = Si, W, Ti, Mn, Sb) for the removal of ^{90}Sr and other key radionuclides from nuclear waste effluents [5–7]. Ion exchange properties of titanium antimonate have been investigated to remove different radionuclides from acidic nuclear waste solutions and in the presence of strongly interfering calcium ions [8]. It was shown that the pyrochlore structure of antimonates could be tuned to the desired ion exchange selectivity by substituting various cations such as W^{6+}, Nb^{5+} into the framework of the parent compound [9]. Recent investigations have shown that carbons obtained by phosphoric acid activation show not only developed porosity but also exhibit significant cation-exchange properties due to acidic surface groups [10]. This phenomenon received only occasional attention in the literature [11–13].

According to the literature, there are no studies describing the possible activation of antimonate surface with phosphoric acid. In this paper, an attempt has been tried to achieve reasonable separation and abstract the radionuclides of ^{134}Cs, ^{60}Co and $^{152+154}Eu$ from strongly various acidic media. This aim can be achieved through preparing silico-antimonate with different Si/Sb ratios and after activation by phosphoric acid.

2. Materials and methods

All chemicals were of analytical grade and used without further purification. ^{134}Cs and $^{152+154}Eu$ isotopes were purchased from Amersham Life Science. ^{60}Co was available by irradiating cobalt nitrate in the Egyptian Reactor Research 2 (ERR2).

2.1. Synthesis of silico-antimonates

SiSb were prepared by dropwise addition of 0.2 M aqueous solutions of Na_2SiO_3 to 0.2 M solutions of Sb-metal (dissolved in aqua regia) in 1:1, 1:2 and 2:1 volume ratios. Gel precipitates were appeared immediately with constant stirring rate at $60 \pm 2\,^{\circ}C$. Part of the gel product which was obtained from the reactants volume ratio1:2 was treated with 100 ml of 3 M H_3PO_4 at 75 °C for one weak. All the reaction products were aged for about two weeks in their mother solutions, decanted, washed with bidistilled water, centrifuged and dried by gentle heating (60 °C). The products were cracked by hot water followed by washing with 0.1 M HNO_3 to be free from Cl^- ions and rewashed with bidistilled water to remove nitrate ions. Finally, the solids were dried at 70 °C in a drying oven, ground, sieved to mesh size 0.225–0.425 mm and stored at room temperature.

* Tel.: +20 2 0105787044; fax: +20 2 0244620784.
E-mail address: ismail_m_ali@yahoo.com.

1385-8947/$ – see front matter © 2009 Elsevier B.V. All rights reserved.
doi:10.1016/j.cej.2009.07.050

2.2. Characterization of the products

The chemical compositions of the solid samples of the obtained SiSb were analyzed using the following techniques. X-ray fluorescence (XRF) was carried out using Phillips X-ray fluorescence model PW 2400 spectrometer. Powder X-ray diffraction was performed using a Shimadzu X-ray diffractometer, XD 610, with a nickel filter and Cu Kα radiation (1.54 Å) operating at 30 kV and 30 mA. Thermal analysis was measured using a Shimadzu DT-60 thermal analyzer, Japan, at a heating rate of 15°/min under a nitrogen atmosphere. The FTIR spectra were acquired in transmission applying KBr disc with a Bomem FTIR spectrometer.

2.3. Equilibrium studies

The distribution coefficient values (K_d) for the studied ions were determined using batch experiments by shaking 0.1 g of SiSb of different forms with 5 ml of 10^{-4} M solution of XCl_n (X = Cs^+, Co^{2+} and Eu^{3+} ions) traced with the respective radioisotope (s). After equilibration (6 h) in a thermostatic shaker water bath at 30, 45 and 60 °C, the mixtures were centrifuged then 1 ml was withdrawn for radiometric assay by measuring the activity level of gamma-rays. A multichannel Analyzer Genie-2000 spectroscopy system (HPGe well type detector) CANBERRA, Inc., USA was used. The distribution coefficients were calculated from the relation:

$$k_d\,(\mathrm{ml/g}) = \frac{A_o - A_{eq}}{A_{eq}}\frac{V}{m} \quad (1)$$

where A_o and A_{eq} are the activities of the tracer in solution before and after equilibrium, respectively, and V/m is the solution volume to adsorbent mass ratio (batch factor, 50 ml/g).

2.4. Column study

Dynamic conditions were conducted to separate radionuclides from their mixture as the following: a column of 0.5 cm internal diameter was packed with 1 g of SiSb (1:2) particles; the bed length (h) of the column was 2 cm and bed volume 1 ml. 500 ml of 10^{-4} M of multi-metal ions preconditioned with 3 M of HNO_3 as representing case of the studied acidic media was used for column saturation. The effluent flow rate was adjusted to be 0.8 bed volume/min. The break-through capacities (mg/g) of the studied ions were measured and calculated from the equation:

$$\text{break-through capacity} = \frac{V_{50\%} Z C_o}{W} \quad (2)$$

where $V_{50\%}$ is the volume at which the ion uptake is 50%, Z is the charge of the ion, C_o is the initial concentration of each element and W is the weight of the column bed (g). Statistical analyses were counted using analysis of variance (ANOVA) procedure [14].

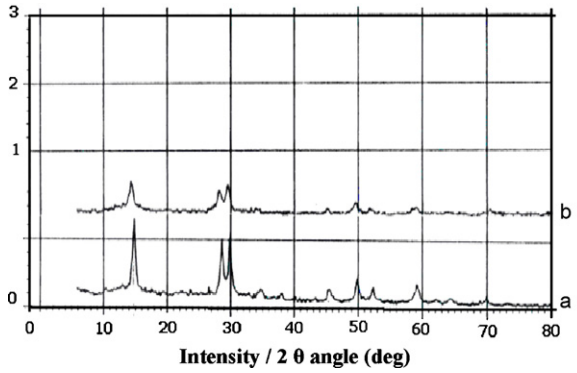

Fig. 1. XRD patterns of non-activated (a) and phosphoric acid activated (b) SiSb (1:2).

3. Results and discussion

3.1. Structural and characterization of silico-antimonates

Conditions for the synthesis and elemental compositions of silico-antimonates are listed in Table 1. The IR, XRD and DTA-TG analyses were carried out to identify the physico-chemical properties of the materials. The FTIR spectra of SiSb (1:2) either that phosphoric acid activated or non-activated (Fig. not shown) indicate that the bands attributed to O–H bonding at 1642 and 3400 cm^{-1} are the main peaks for all materials [7]. New spectral band at 1185 cm^{-1} in the case of phosphoric acid activated SiSb was observed. This band is attributed to the phosphate group [8]. The presence of phosphate group was also quantitively confirmed from XRF measurements as given in Table 1.

The observed reflections and relative intensities in the XRD pattern of non-activated SiSb (1:2) (Fig. 1a) were consistent with cubic structure of antimony oxide [15]. However, material prepared at Si:Sb ratio of 1:2 then activated with phosphoric acid exhibited minor decrease for most peak intensities with no 2θ changes (Fig. 1b). Accordingly, slightly distortion in the cubic structure seems to be occurred during the activation processing. Similar behavior was reported for most phosphate incorporated materials [16].

A simultaneous DTA/TG thermal analysis of silico-antimonate samples was carried out (curves not given). The data show that the dehydration reaction of SiSb (1:2) is appeared at two endothermic peaks (89 and 292 °C) which corresponding to a total water content of 10 mol. However, the dehydration reaction of phosphated SiSb (1:2) is appeared as two endothermic peaks at 94 and broad one at 300 °C with a total water content of 11 mol. Such behaviors may be indicating, higher thermal stability and water content of the activated silico-antimonate compared to the non-activated one. Therefore, in aqueous media it can be expected that the activated form of silico-antimonate has surface hydroxyl and phosphate groups which are more available to react with the positive metal ions.

Table 1
Synthesis and properties of silico-antimonates.

Silico-antimonate[a]	0.3 M Si:0.3 M Sb:3 M H_3PO_4 reactants volume, ml	Si/Sb mole ratio in product	Color	XRD	% Water content
SiSb(2:1)	200:100:–	0.41	White	Crystalline	19.50
SiSb(1:1)	100:100:–	0.37	White	Crystalline	19.00
SiSb(1:2)	100:200:–	0.29	White	Crystalline	19.20
SiSb(1:2)/H_3PO_4	100:200:100	0.20	White	Crystalline	20.00

[a] Empirical formula of silico-antimonates by XRF (using oxides list); SiSb (2:1) $(Na_2O)_{0.3}(SiO_2)_{1.9}(Sb_2O_3)_{2.3}\cdot 11H_2O$; SiSb (1:1) $(Na_2O)_{0.3}(SiO_2)_{2.6}(Sb_2O_3)_{3.5}\cdot 15H_2O$; SiSb (1:2) $(Na_2O)_{0.3}(SiO_2)_{1.4}(Sb_2O_3)_{2.4}\cdot 10H_2O$; SiSb (1:2)/$H_3PO_4$ $(Na_2O)_{0.3}(SiO_2)_{1.0}(Sb_2O_3)_{2.4}(P_2O_5)_{0.15}\cdot 11H_2O$.

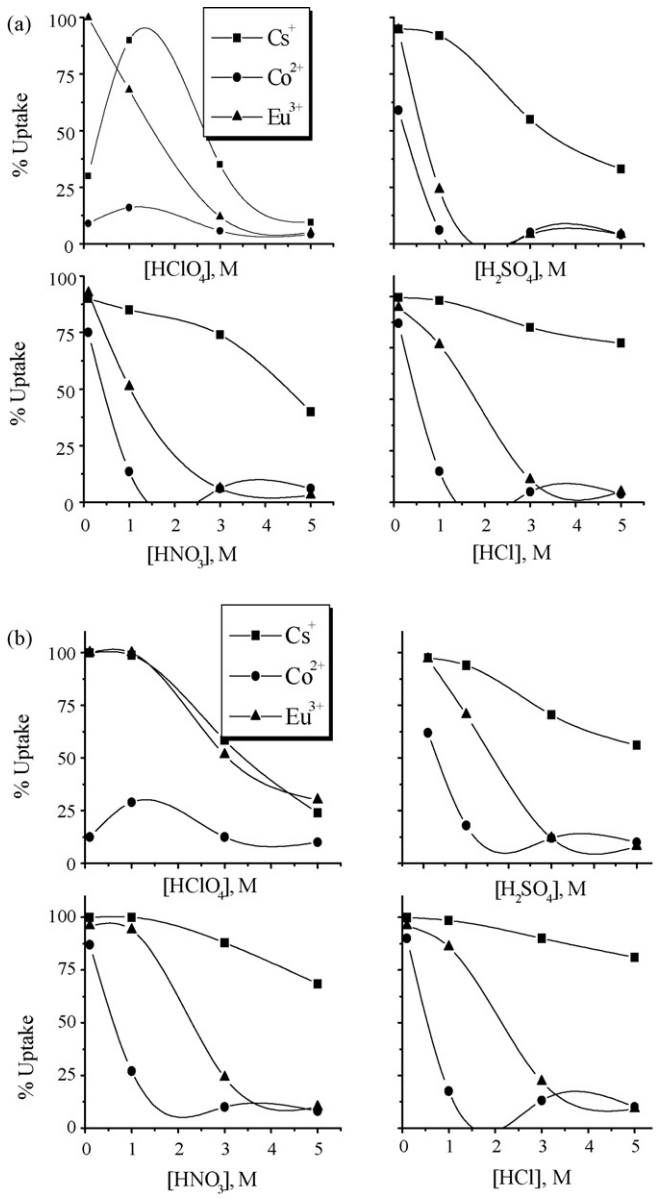

Fig. 2. % Uptake of Cs^+, Co^{2+}, and Eu^{3+} ions from $HClO_4$, H_2SO_4, HNO_3 and HCl on (a) non-activated and (b) phosphoric acid activated SiSb (1: 2) at 30 ± 1 °C.

3.2. Influence of acidity on the ions uptake

The equilibrium uptake of co-exiting ^{134}Cs, ^{60}Co and $^{152+154}Eu$ on non- and activated-silico-antimonates from different acidic media was carried out. The effects of acid types including $HClO_4$, HNO_3, HCl and H_2SO_4 at acid concentration ranging from 0.1 to 5 M on the uptake percent are presented in Fig. 2a and b. The equilibrium sorption data shown in Fig. 2 indicate that: (i) at the low acid concentration the metal cations exhibit generally strong uptake and high affinity with the antimonate matrix. This behavior is a prominent for many sorption processes. Only two unexpected low sorption cases at 0.1 M $HClO_4$ (Cs^+/SiSb unmodified and Co^{2+}/SiSb unmodified) were detected, perhaps due to ions hydrolysis at this low acid concentration. However, with increasing acid concentration the H^+ increase and further competes the exchange sites. This behavior indicates that the ion exchange equilibrium shown in Eq. (3) is predominant in backward direction with the increase in acid concentration:

$$n\text{R–H (exchange)} + \text{M}^{n+}\text{ (aqueous)} \rightleftharpoons \text{R–M} + n\text{M}^{+} \quad (3)$$

(ii) within the studied acid concentrations range the sorption of cations in majority follows the selectivity order; $Cs^+ > Eu^{3+} \gg Co^{2+}$. The hydrated ionic radius was regarded to play a major role affecting on many of these selectivity behavior. However, in minor cases and at different acid concentration the selectivity order $Eu^{3+} > Cs^+ \gg Co^{2+}$ was reported (Fig. 2). This result of non-comparable selectivity trend thus not relevant to one factor but it may be attributed to other factors affect on the cations. Based on the results of K_d values, separation performance of the ions was reported at selected conditions. For example; at 0.1 M $HClO_4$, separation of Eu^{3+} (K_d = 49,950) from Cs^+ (K_d = 21) and Co^{2+} (K_d = 5) can be achieved using SiSb (1:2). While, separation of Cs^+ (K_d = 49, 950 and 3284) from Co^{2+} (K_d = 450 and 11) and Eu^{3+} (K_d = 1200 and 283) can be achieved at 0.1 and 5 M of HCl on the activated SiSb, respectively. Also, separation of Cs^+ (K_d = 5E6) from Co^{2+} (K_d = 335 and 18) and Eu^{3+} (K_d = 616 and 51) at 0.1 and 1 M HNO_3 on the activated SiSb can be achieved, respectively; (iii) under identical conditions, activated SiSb tend to possess higher ions uptake compared to the non-activated one. This important feature may be due the increased amount of strongly acidic phosphorous-containing surface groups. Puziy et al. [17] reported that, synthetic carbons activated with phosphoric acid are the most important for the adsorption of heavy metals from acid solutions. Phosphate anions were also used to generate acidic properties through the impregnation with TiO_2 and/or sol–gel silica [18,19]. In addition, it can be assumed that a relatively change in the unit cell dimensions of the cubic SiSb phosphated form (change to poor crystalline phase) leads to a significant enhancement of its sorption efficiency. Further, the high in ions affinity of the activated SiSb may be attributed to it posses slightly higher number of the structural water molecules (11 mol) compared to the non-activated one (10 mol) (Table 1). An increasing the amount of water content provides the material with high porous feature as well as more of localized protons [6]. These two factors may enhance the ion exchange affinity if the hydration reaction of the SiSb structure OH^- groups is considered. When these –OH groups are hydrated, the protons in the form of hydronium ions (H_3O^+) either on the surface or inside the pores can easily move to be responsible for the ion exchange process.

3.3. Kinetic studies

Batch experiments were conducted to explore the sorption rate of 10^{-4} M of Cs^+, Co^{2+} and Eu^{3+} on the SiSb (1:2) at V/m = 50 ml/g, 0.1 M of each $HClO_4$, HNO_3, HCl and H_2SO_4 and at 30 ± 1 °C. Plotting the uptake percent against time indicated that the rate of sorption of Eu^{3+} in $HClO_4$ is relatively fast and the equilibrium is reached within 60 min achieving 99% followed by Cs^+ at 6 h with 30% and finally Co^{2+} at 6 h with 9% uptake. However, in the case of H_2SO_4, HNO_3 and HCl the rate of sorption of Cs^+ (>90%) and Eu^{3+} (>90%) by SiSb (1:2) is quite rapid followed by Co^{2+} (60% uptake). This relative fast rate either for Cs^+ or Eu^{3+} ions is certainly related to the availability of active sites on SiSb surface. Due to no significant sorption was observed after 6 h, the contact time adjusted to be 6 h to ensure complete equilibrium for subsequent experiments.

The process of ions removal from acidic media was studied kinetically applying two kinetic models. The pseudo-first-order rate model which can be expressed as [20]:

$$\log(q_e - q_t) = \log q_e - \left(\frac{K_1}{2.303}\right) t \quad (4)$$

where q_e and q_t are the amounts of metal ions sorbed at equilibrium and at time t, respectively (both in mg of metal ions/g of sorbent), K_1 is the overall rate constant (1/min) and q_e can be calculated using

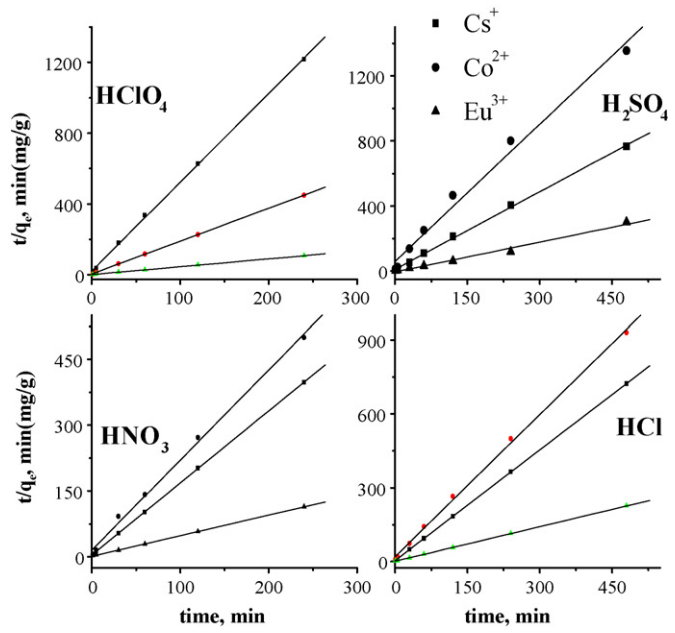

Fig. 3. Pseudo-second-order model of Cs^+, Co^{2+}, and Eu^{3+} sorption on SiSb (1: 2) from different acid media (0.1 M) at 30 ± 1 °C.

the following relationship:

$$q_e = \frac{(C_o - C_e)}{m} \times V \quad (5)$$

where C_o and C_e are the initial and the equilibrium metal ion concentrations (mg/l), V is the volume of aqueous phase and m is the amount of the SiSb used (g). Applying this model performs less well fit to the experimental data (correlation coefficient values <0.9). Another model including the pseudo-second-order kinetic model [21,22] was used to predict the kinetic parameters:

$$\frac{t}{q_t} = \frac{1}{K_2 q_e^2} + \frac{t}{q_e} \quad (6)$$

Fig. 3 shows the relation of t/q_t against t for ion exchange reactions on SiSb (1:2) from different acid media. The second-order rate constant K_2 (g mg^{-1} min^{-1}) and q_e (mg/g) were determined from the intercept and slope and their values are given in Table 2. The model is best fitted with the experimental data and all correlation coefficients are >0.99. This model based on the assumption that the rate-determining step may be a chemo-sorption involving valence forces through sharing or exchange of electrons between the ions and the exchanger [22].

Table 2
The pseudo-second-order rate constants of 10^{-4} M of Cs^+, Co^{2+} and Eu^{3+} on SiSb (1:2) in different acid media of 0.1 M concentrations.

Acid	Metal ions	q_e (mg/g) exp[a]	Pseudo-second-order kinetic model		
			q_e (mg/g) cal[b]	Rate constant	R^2
$HClO_4$	Cs^+	0.200	0.199	1.15	0.980
	Co^{2+}	0.055	0.054	0.74	0.980
	Eu^{3+}	2.280	2.250	0.44	0.980
H_2SO_4	Cs^+	0.627	0.628	0.24	0.998
	Co^{2+}	0.355	0.357	1.32	0.988
	Eu^{3+}	2.15	1.640	0.07	0.986
HNO_3	Cs^+	0.603	0.610	0.63	0.998
	Co^{2+}	0.455	0.487	0.28	0.996
	Eu^{3+}	2.11	2.120	0.19	0.999
HCl	Cs^+	0.663	0.666	0.52	1.000
	Co^{2+}	0.528	0.520	0.18	0.998
	Eu^{3+}	2.159	2.170	0.13	1.000

[a] Experimental.
[b] Calculated.

Table 3
The equilibrium sorption capacity for Cs^+, Co^{2+} and Eu^{3+} on non- and activated-SiSb (1:2) in 3 M acid concentration at different reaction temperatures.

Acid	Metal ions	Equilibrium sorption capacity (mg/g)					
		Non-activated SiSb (1:2)			Activated SiSb (1:2)		
		303 K	318 K	333 K	303 K	318 K	333 K
$HClO_4$	Cs^+	0.170	0.180	0.190 [a]	0.220	0.220	0.230 [b]
	Co^{2+}	0.020	0.022	0.030 [a]	0.030	0.033	0.034 [a]
	Eu^{3+}	0.150	0.230	0.340 [a]	0.430	0.480	0.540 [a]
H_2SO_4	Cs^+	0.250	0.240	0.230 [c]	0.360	0.380	0.410 [a]
	Co^{2+}	0.040	0.030	0.024 [c]	0.023	0.044	0.054 [a]
	Eu^{3+}	0.080	0.080	0.082 [b]	0.157	0.200	0.240 [a]
HNO_3	Cs^+	0.380	0.400	0.420 [a]	0.490	0.480	0.480 [b]
	Co^{2+}	0.020	0.020	0.022 [b]	0.030	0.040	0.045 [a]
	Eu^{3+}	0.084	0.120	0.200 [a]	0.440	0.049	0.520 [a]
HCl	Cs^+	0.540	0.500	0.400 [c]	0.520	0.500	0.510 [b]
	Co^{2+}	0.023	0.023	0.025 [b]	0.031	0.040	0.046 [a]
	Eu^{3+}	0.140	0.220	0.320 [a]	0.730	0.770	0.800 [a]

[a] Increase.
[b] Not effect.
[c] Decrease.

3.4. Effect of temperature

It is known that, if sorption is governed only by physical phenomena, an increase in temperature will be followed by a decrease in sorption capacity [23]. Accordingly, the effect of temperature ranged from 303 to 333 K on the sorption of Cs^+, Co^{2+} and Eu^{3+} at concentration level of 10^{-4} M onto both non- and activated-SiSb (1:2) in various acid media was studied. The results show that the equilibrium capacity of the phosphoric acid-activated SiSb (1:2) is higher than that of the non-activated one as reported in Table 3. In most cases, it can be seen that the equilibrium capacity increased with the temperature increasing. Thus, chemisorptions play the main role in the ions uptake on antimonate surface. For example, it was found that the equilibrium sorption capacities for europium at 303, 318 and 333 K (in 3 M $HClO_4$) are 0.15, 0.23 and 0.34 mg/g on SiSb (1:2) and 0.43, 0.48 and 0.54 mg/g on activated SiSb respectively. The effect of temperature on sorption process was further analyzed by Van't Hoff plots based on the equation:

$$\ln K_d = \frac{\Delta S^\circ}{2.303R} - \frac{\Delta H^\circ}{2.303\,RT} \quad (7)$$

where the K_d is the distribution coefficient, T (K) is the absolute temperature, R is the gas constant (8.314 J/(mol K)), ΔS° is the entropy change (J/mol) and ΔH° is the enthalpy change (kJ/mol). The values of ΔH° and ΔS° could be obtained from the linear plots of $\ln K_d$ against $1/T$ for the studied cations. ΔG° values were computed at each temperature by the relation (8):

$$\Delta G^\circ = \Delta H^\circ - T\,\Delta S^\circ \quad (8)$$

The thermodynamic values of Cs^+, Co^{2+} and Eu^{3+} sorption on both non- and activated-SiSb in 3 M of different studied acid media were reported in Table 4. The estimated enthalpy changes for most of the studied systems are positive which indicate that the processes are endothermic in nature. Spontaneity of the sorption system was demonstrated by the negative values of ΔG°. The mean values of ΔG° were found to vary from −1.29 for Co^{2+}/SiSb/$HClO_4$/303 K-system to −13.1 kJ/mol for Cs^+/SiSb/HCl/303 K-system. Also, the ΔG° were found to vary from −1.95 for Co^{2+}/activated SiSb/H_2SO_4/303 K-system to −13.92 kJ/mol for Cs^+/activated SiSb/HCl/333 K-system. More negativity of ΔG°values for the activated-SiSb compared to the

Table 4
Thermodynamic parameters for sorption of 10^{-4} M of Cs^+, Co^{2+} and Eu^{3+} on non- and activated-SiSb (1:2) in 3 M acid concentration.

Acid	Metal ions	SiSb (1:2)					Activated-SiSb (1:2)				
		ΔH° (kJ/mol)	ΔS° (J/Kmol)	$-\Delta G^\circ$ (kJ/mol)			ΔH° (kJ/mol)	ΔS° (J/Kmol)	$-\Delta G^\circ$ (kJ/mol)		
				303 K	318 K	333 K			303 K	318 K	333 K
$HClO_4$	Cs^+	4.65	38.82	7.11	7.69	8.27	2.41	36.6	8.6	9.32	9.77
	Co^{2+}	10.55	39.1	1.29	1.88	2.47	6	52.96	10.0	10.84	11.63
	Eu^{3+}	24.27	90.87	3.26	4.62	5.99	8.06	47.14	6.22	6.93	7.63
H_2SO_4	Cs^+	−3.9	15.29	8.53	8.76	8.99	7.06	57.6	10.39	11.25	12.12
	Co^{2+}	−17.54	−46.5	3.45	2.75	2.05	25	88.95	1.95	3.28	4.62
	Eu^{3+}	3.3	15.3	1.33	1.56	1.79	13.72	55.7	3.15	3.99	4.82
HNO_3	Cs^+	6.9	57.36	10.48	11.34	12.2	4.4	26.77	3.71	4.11	4.51
	Co^{2+}	1.33	9.47	1.53	1.68	1.82	10.72	43.9	2.58	3.24	3.89
	Eu^{3+}	16.54	62.6	2.42	3.36	4.30	5.5.0	39.1	6.34	6.93	7.52
HCl	Cs^+	−27.43	47.38	13.1	12.36	11.6	−2.99	32.84	12.94	13.43	13.92
	Co^{2+}	2.49	13.88	1.71	1.92	2.91	11.89	47.38	9.46	10.84	11.63
	Eu^{3+}	24.9	92.36	3.10	4.47	5.85	4.07	39.65	7.94	7.93	7.63

non-activated one (Table 4) confirms not only the more stability of the systems but also the positive role of the activation process. Negativity confirms also the high preferring of the activated silico-antimonate for the studied ions compared to the protons. In most cases, $\Delta G^\circ_{318\,K}$ values were decreased with increasing reaction temperature. This confirms that the reaction is favored at high temperature which indicates to an entropy-producing process prevails in the M^{n+}/H^+ exchange system as established in Eq. (3). Such mechanism was proposed earlier by Zakaria et al. for the adsorption of Gd^{3+}, Ce^{3+} and Eu^{3+} ions on titanium (IV) antimonate [24].

3.5. Effect of Si:Sb ratios on the sorption of ions

The ^{134}Cs, ^{60}Co and $^{152-154}Eu$ sorption percent on SiSb at different Sb^{5+}/Si^{4+} ratios was determined in 1 M HNO_3 medium and the results are shown in Fig. 4. The results indicated that, silico-antimonate of high antimony content (SiSb 1:2) reveals the highest sorption affinity compared to that obtained from the other ratios. This indicates that with increasing the ratio of Sb^{5+}/Si^{4+} in the reactants the acidity of the antimonate product increases. Therefore, an increase in the electrostatic interaction of cations to be exchanged with the sorption sites is strongly expected [25]. The data presented so far indicate that the modified SiSb (1:2) has two advantages as sorbent. The first is that it possesses the highest Sb^{5+} content among the studied antimonates where the other was gained when activated by phosphoric acid. Thus the modified antimonate reflects an improved removal performance as well as it can be regarded as a promising material in the separation of radionuclides from acidic solutions.

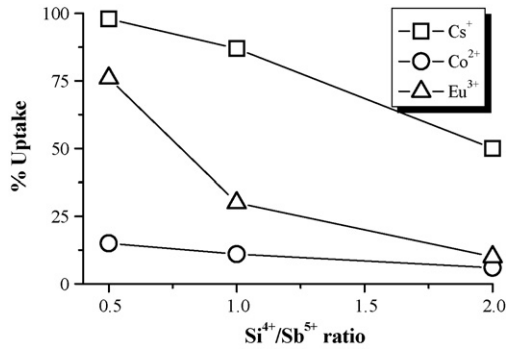

Fig. 4. % Uptake of Cs^+, Co^{2+} and Eu^{3+} ions from 1 M HNO_3 on silico-antimonate of different Si^{4+}/Sb^{5+} reactant ratios at 30 ± 1 °C.

3.6. Dynamic sorption study

In this study, 500 ml of 3 M HNO_3 solution containing a mixture of 10^{-4} M of each studied ions was passed through a glass column packed with 1 g of SiSb (1:2) at a flow rate 0.8 bed volume/min. Break-through capacities (Q_e) of ^{134}Cs, ^{60}Co and $^{152+154}Eu$ radionuclides on SiSb (1:2) were calculated from their corresponding curves shown in Fig. 5a. It was found that the break-through capacities are 0.67, 0.036 and 0.15 mg/g for Cs, Co and Eu ions, respectively. The values of Q_e were compared with the respective values at similar batch condition experiments that reported in Table 3. It was found that the Q_e values are higher than those obtained from batch experiments. This behavior could be attributed to the insufficient ions required for saturation in case of batch operation. Consequently, Fig. 5b shows the separation profile of ^{134}Cs from ^{60}Co and $^{152+154}Eu$ radionuclides adsorbed on SiSb (1:2) column. By using 1 M of HNO_3 as eluent, release of any of the isotopes not observed. However, ^{134}Cs was released when 5 M of HNO_3 was used. This behavior is accepted because the Cs^+ ion shows the highest sorption on the SiSb column compared to the other ions.

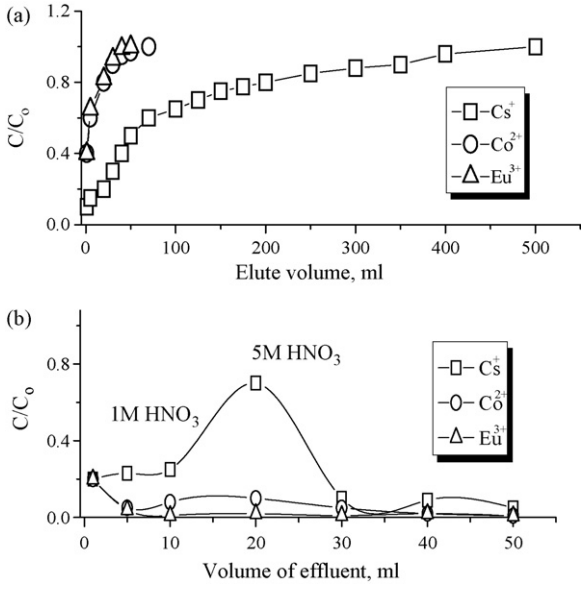

Fig. 5. (a) Break-through curves of Cs^+, Co^{2+} and Eu^{3+} ions from 3 M HNO_3 on SiSb (1:2) at 30 °C (0.5 cm diameter, 2 cm length and 0.8 ml/min flow rate). (b) Elution curves of mixture of Cs^+, Co^{2+} and Eu^{3+} ions by HNO_3 from SiSb (1:2) (0.5 cm diameter, 2 cm length and 0.8 ml/min flow rate).

4. Conclusion

The silico-antimonates synthesized in this work have cubic structure analogues of the antimony pentoxide. Several factors may be affecting the ion exchange properties of the materials in question such as, water content, surface acidity as well as the elemental composition. Slightly distortion in the cubic structure of silico-antimonate was found to be occurred due to the phosphoric acid activation process. The sorption efficiency for Cs^+ and Eu^{3+} ions from high acid media (up to 3 M) of $HClO_4$, H_2SO_4, HNO_3 and HCl was found to be increased by the activation process. Kinetic parameters show better fit using pseudo-second-order model for sorption of Cs, Co and Eu ions into silico-antimonate. Increasing the amount of Sb^{5+} in the SiSb material yields an enhancement of the metal ions affinity while the more negative values of ΔG° reveal a positive role of phosphoric acid in the sorption process. Silico-antimonate of high antimony content (SiSb 1:2) and after activation with phosphoric acid is expected to be the highest and promising for Cs^+ and Eu^{3+} separation at elevated acidic conditions.

Acknowledgements

The author is deeply indebted to Prof. H. Aly and Prof. I. El-Naggar for their encouragements.

Appendix A. Supplementary data

Supplementary data associated with this article can be found, in the online version, at doi:10.1016/j.cej.2009.07.050.

References

[1] H. Park, I. Kim, H. Kim, S. Ryu, J. Kim, Immobilization of molten salt waste into $MZr_2(PO_4)_3$ (M = Li, Na, Cs, Sr), J. Radioanal. Nucl. Chem. 268 (2006) 617–626.
[2] I. El-Naggar, E. Zakaria, I. Ali, Aspects of the adsorption behavior of Cu^{2+}, Zn^{2+} and Ni^{2+} ions on lithium titanate ion exchanger, Sep. Sci. Technol. 39 (4) (2004) 959–974.
[3] I. Ali, E. Zakaria, I. El-Naggar, Radiotracer study on the adsorption of Cs-134 on stannic silicate ion exchanger, Arab. J. Nucl. Sci. 37 (2) (2004) 31–42.
[4] E. Zakaria, I. Ali, H. Aly, Adsorption behavior of ^{134}Cs and ^{22}Na ions on tin and titanium ferrocyanides, Adsorption 10 (2004) 45–58.
[5] M. Webb, S. Ward, S. Amin, Metal antimonates – highly effective ion exchangers for radionuclide removal from acidic and neutral waste solutions, in: WM'01 Conf., February 25–March 1, Tucson, AZ, 2001.
[6] T. Moller, A. Clearfield, R. Harjula, Preparation of hydrous metal of Sb, Si, Ti and W with a pyrochlore structure and exchange of radioactive cesium strontium into the materials, Micropor. Mesopor. Mater. 54 (2002) 187–199.
[7] H.F. Aly, I.M. El-Nagger, Synthesis of tetravalent metal antimonates: characteristics and use in treatment of radioactive waste solutions, J. Radioanal. Nucl. Chem. 228 (1998) 151–160.
[8] I. Yamagishi, Y. Morita, M. Kubota, M. Tsuji, Ion exchange selectivity for Am^{3+}, Nd^{3+} and Eu^{3+} on titanium antimonate and their chromatographic separation, Radiochim. Acta 75 (1996) 27–32.
[9] T. Moller, R. Harjula, P. Kelokaski, K. Vaaramaa, P. Karhu, J. Lehto, Titanium antimonates in various Ti:Sb ratios: ion exchange properties for radionuclide ions, J. Mater. Chem. 13 (2003) 535–543.
[10] A. Puziy, O. Poddubnaya, A. Ziatdinov, On the chemical structure of phosphorus compounds in phosphoric acid-activated carbon, Appl. Surf. Sci. 252 (23) (2006) 8036–8038.
[11] C.A. Toles, W.E. Marshall, M.M. Johns, Surface functional groups on acid-activated nutshell, Carbons 37 (8) (1999) 1207–1214.
[12] C.A. Toles, W.E. Marshall, M.M. Johns, Phosphoric acid activation of nutshells for metals and organic remediation: process optimization, J. Chem. Technol. Biotechnol. 72 (1998) 255–263.
[13] A. Puziy, O. Poddubnaya, Surface acidity of synthetic carbons activated with phosphoric acid, in: Eurocarbon'98, Strasbourg, France, 1998, p. 449.
[14] Williams, Wilkins, Clinical Epicochemiology and Biostatistics, Baltimore, Maryland, USA, 1992.
[15] Powder diffraction card 33-1018, Joint committee on powder diffraction standards JCPDS-ICDD, USA, 1995.
[16] B. Pan, Q. Zhang, W. Zhang, B. Pan, W. Du, L. Lv, Q. Zhang, Z. Xu, Q. Zhang, Highly effective removal of heavy metals by polymer-based zirconium phosphate: a case study of lead ion, J. Colloid Interface Sci. 310 (2007) 99–105.
[17] A. Puziy, O. Poddubnaya, A. Alonso, F. Garcia, J. Tascon, Synthetic carbons activated with phosphoric acid I. Surface chemistry and ion binding properties, Carbon 40 (2002) 1493–1505.
[18] K. Parida, M. Acharya, S. Samantaray, T. Mishra, Studies on anion promoted titania I: preparation, characterization and catalytic activity towards alcohol and cumene conversion reactions of phosphated titania, J. Colloid Interface Sci. 217 (1999) 388–394.
[19] M.E. Manrı Quez, T. Lo Pez, R. Gomez, M. Picquart, J.G. HernaïNdez-Cortez, Sol–gel silica modified with phosphate and sulfate ions, J. Non-Cryst. Solids 345 (2004) 643–650.
[20] C. Weng, C. Huang, Adsorption characteristic of Zn(II) from dilute aqueous solution by fly ash, Colloid Surf. A 247 (2004) 137–146.
[21] Y. Ho, Adsorption of heavy metals from waste streams by peat, PhD thesis, Univ. of Birmingham, UK, 1995.
[22] Y. Ho, S. McKay, Pseudo-second order model for sorption process, Biochemistry 34 (1999) 451–465.
[23] F. Habashi, A Text book of Hydrometallurgy, Metallurge Extractive Quebec, Enr. Que., Canada, 1993.
[24] E. Zakaria, I. Ali, I. El-Naggar, Thermodynamic and ion exchange equilibria of Gd^{3+}, Eu^{3+} and Ce^{3+} ions on H-form of titanium (IV) antimonate, Colloids Surf. A 210 (2002) 33–40.
[25] K. Varshney, G. Gupta, Tin (IV) antimonate as a lead-selective cation exchanger: synthesis, characterization and analytical applications, Bull. Chem. Soc. Jpn. 63 (1990) 1515–1520.